Supporting Information

Section S1. COVID-19 Epidemic Model Structure and Parameters

The model structure is diagrammed in Fig. S1 and described in the equations below. For each age and risk group, we build a separate set of compartments to model the transitions between the states: susceptible (*S*), exposed (*E*), symptomatic infectious (I^Y), asymptomatic infectious (I^A), symptomatic infectious that are hospitalized (I^H), recovered (*R*), and deceased (*D*). The symbols *S, E,* I^Y, I^A, I^H, *R*, and *D* denote the number of people in that state in the given age/risk group and the total size of the age/risk group is $N = S + E + I^Y + I^A + I^H + R + D$.

The model for individuals in age group *a* and risk group *r* is given by:

$$\frac{dS_{a,r}}{dt} = -\sum_{i\in A}\sum_{j\in K}\left(I^Y_{i,j}\omega^Y + I^A_{i,j}\omega^A + E_{i,j}\omega^E\right)\beta\phi_{a,i}/N_i$$

$$\frac{dE_{a,r}}{dt} = \sum_{i\in A}\sum_{j\in K}\left(I^Y_{i,j}\omega^Y + I^A_{i,j}\omega^A + E_{i,j}\omega^E\right)\beta\phi_{a,i}/N_i - \sigma E_{a,r}$$

$$\frac{dI^A_{a,r}}{dt} = (1-\tau)\,\sigma E_{a,r} - \gamma^A I^A_{a,r}$$

$$\frac{dI^Y_{a,r}}{dt} = \tau\sigma E_{a,r} - (1-\pi)\,\gamma^Y I^Y_{a,r} - \pi\eta I^Y_{a,r}$$

$$\frac{dI^H_{a,r}}{dt} = \pi\eta I^Y_{a,r} - (1-\nu)\,\gamma^H I^H_{a,r} - \nu\mu I^H_{a,r}$$

$$\frac{dR_{a,r}}{dt} = \gamma^A I^A_{a,r} + (1-\pi)\,\gamma^Y I^Y_{a,r} + (1-\nu)\,\gamma^H I^H_{a,r}$$

$$\frac{dD_{a,r}}{dt} = \nu\mu I^H_{a,r}$$

where *A* and *K* are all possible age and risk groups, ω^A, ω^Y, ω^H are relative infectiousness of the I^A, I^Y, E compartments, respectively, β is transmission rate, $\phi_{a,i}$ is the mixing rate between age group a, $i \in A$, γ^A, γ^Y, γ^H are the recovery rates for the I^A, I^Y, I^H compartments, respectively, σ is the exposed rate, τ is the symptomatic ratio, π is the proportion of symptomatic individuals requiring hospitalization, η is rate at which hospitalized cases enter the hospital following symptom onset, ν is mortality rate for hospitalized cases, and μ is rate at which terminal patients die.

We model stochastic transitions between compartments using the τ-leap method[1,2] with key parameters given in Table S1. Assuming that the events at each time-step are independent and do not impact the underlying transition rates, the numbers of each type of event should follow Poisson distributions with means equal to the rate parameters. We thus simulate the model according to the following equations:

$$S_{a,r}(t+1) - S_{a,r}(t) = -P_1$$

$$E_{a,r}(t+1) - E_{a,r}(t) = P_1 - P_2$$

$$I^A_{a,r}(t+1) - I^A_{a,r}(t) = (1-\tau)\,P_2 - P_3$$

$$I^Y_{a,r}(t+1) - I^Y_{a,r}(t) = \tau P_2 - P_4 - P_5$$

$$I^H_{a,r}(t+1) - I^H_{a,r}(t) = P_5 - P_6 - P_7$$

$$R_{a,r}(t+1) - R_{a,r}(t) = P_3 + P_4 + P_6$$
$$D_{a,r}(t+1) - D_{a,r}(t) = P_7 \ ,$$

with

$$P_1 \sim Pois\left(S_{a,r}(t) F_{a,r}(t)\right)$$
$$P_2 \sim Pois\left(\sigma E_{a,r}(t)\right)$$
$$P_3 \sim Pois\left(\gamma^A I^A_{a,r}(t)\right)$$
$$P_4 \sim Pois\left((1-\pi)\gamma^Y I^Y_{a,r}(t)\right)$$
$$P_5 \sim Pois\left(\pi\eta I^Y_{a,r}(t)\right)$$
$$P_6 \sim Pois\left((1-\nu)\gamma^H I^H_a\right)$$
$$P_7 \sim Pois\left(\nu\mu I^H_{a,r}(t)\right)$$

and where $F_{a,r}$ denotes the force of infection for individuals in age group *a* and risk group *r* and is given by: $F_{a,r}(t) = \sum_{i \in A} \sum_{j \in K} \left(I^Y_{i,j}(t)\omega^Y + I^A_{i,j}(t)\omega^A + E_{i,j}(t)\omega^E \right) \beta_{a,i}\Phi_{a,i}/N_i$

Fig S1. Compartmental model of COVID-19 transmission in a US city

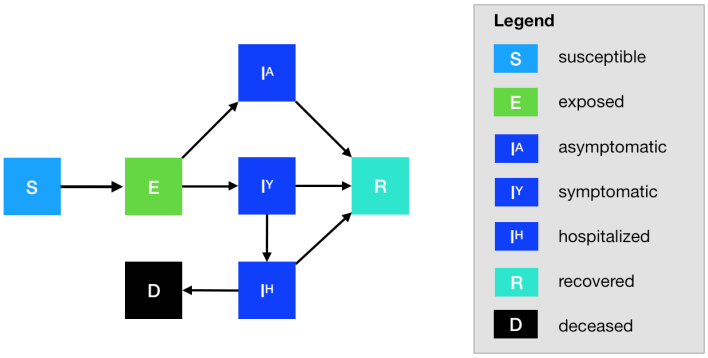

Each subgroup (defined by age and risk) is modeled with a separate set of compartments. Upon infection, susceptible individuals (*S*) progress to exposed (*E*) and then to either symptomatic infectious (I^Y) or asymptomatic infectious (I^A). All asymptomatic cases eventually progress to a recovered class where they remain protected from future infection (*R*); symptomatic cases are either hospitalized (I^H) or recover. Mortality (*D*) varies by age group and risk group and is assumed to be preceded by hospitalization.

Table S1.1. Initial conditions, school closures and social distancing policies

Variable	Settings
Initial day of simulation	3/1/2020
Initial infection number in locations	5 symptomatic cases in 18-49y age group
Trigger to close school	3/14/2020
Closure Duration	Until start of 2020-2021 school year (8/17/20)
α: Reduction of non-household contacts (work and other)	Five scenarios: [0, .25, 0.5, .75, 0.9]
Age-specific and day-specific contact rates	Home, work, other and school matrices provided in Tables S1.4-S1.7 Normal weekday = home + work + other + school Normal weekend = home + other Normal weekday holiday = home + other Normal weekday during summer or winter break = home + work + other School closure weekday = home + (1-α)*(work + other) School closure weekend = home + (1-α)*(other) School closure weekday holiday = home + (1-α)*(other) School closure during summer or winter break = home + (1-α)*(work + other)

Table S1.2. Model parameters. Values given as five-element vectors are age-stratified with values corresponding to 0-4, 5-17, 18-49, 50-64, 65+ year age groups, respectively.

Parameters	Best guess - values (doubling time = 7.2 days)	Best guess values (doubling time = 4 days)	Source
R_0	2.2	2.2	Li et al. [3]
δ : doubling time	7.2 days	4 days	Kraemer et al. [4]
β : transmission rate	0.01622242	0.02599555	Fitted[a] to obtain specified R_0 given δ
γ^A : recovery rate on asymptomatic compartment	Equal to γ^Y		
γ^Y : recovery rate on symptomatic non-treated compartment	$\frac{1}{\gamma^Y} \sim \ Triangular\,(21.2, 22.6, 24.4)$		Verity et al. [5]
τ : symptomatic proportion (%)	82.1		Mizumoto et al. [6]
σ : exposed rate	$\frac{1}{\sigma} \sim \ Triangular\,(5.6, 7, 8.2)$		Lauer et al. [7]
P: proportion of pre-symptomatic (%)	12.6		Du et al. [8]
ω^E : relative infectiousness of infectious individuals in compartment E	$\omega^E = \frac{\left(\frac{\gamma^Y IHR}{\eta} + \frac{1-\gamma^Y IHR}{\gamma^Y}\right)\omega^Y \sigma P}{1-P}$		
ω^A : relative infectiousness of infectious individuals in compartment I^A	0.4653		Set to mean of ω^E
IFR: infected fatality ratio, age specific (%)	Overall: [0.0016, 0.0049, 0.084, 1.000, 3.371] Low risk: [0.00091668, 0.0021789, 0.03388, 0.25197, 0.64402]		Age adjusted from Verity et al. [5]

	High risk: [0.009167, 0.02179, 0.33878, 2.5197, 6.4402]	
YFR: symptomatic fatality ratio, age specific (%)	Overall: [0.001949, 0.006025, 0.10265, 1.2182, 4.10657] Low risk: [0.0011165, 0.002654, 0.04126, 0.3069, 0.78443] High risk: [0.01117, 0.02654, 0.4126, 3.06903, 7.8443]	$YFR = \frac{IFR}{1-\tau}$
h: high-risk proportion, age specific (%)	[8.2825, 14.1121, 16.5298, 32.9912, 47.0568]	Estimated using 2015-2016 Behavioral Risk Factor Surveillance System (BRFSS) data with multilevel regression and poststratification using CDC's list of conditions that may increase the risk of serious complications from influenza [9–11]
rr: relative risk for high risk people compared to low risk in their age group	10	Assumption
School calendars	Austin Independent School District calendar (2019-2020, 2020-2021) [12]	

[a]The parameter β is fitted through constrained trust-region optimization in SciPy/Python [13]. Given a value of β, a deterministic simulation is run based on central values for each parameter, from which we can compute the implied $\overline{R_0}(\beta)$. We (1) track the daily number of new cases I_t (both symptomatic and asymptomatic) during the exponential growth portion of the epidemic, (2) compute the log of the number of new cases: $y_t = log(I_t)$ and (3) use least squares to fit a line to this curve: $\log log\ (I_t) = y_0 + g \cdot t$. We then estimate the reproduction number $\overline{R_0}(\beta)$ of the simulation for that specific value of β as $\overline{R_0}(\beta) = \Gamma \cdot g +$ 1 where Γ is the generation time given by $\Gamma = \frac{\delta(R_0 - 1)}{\log log\,(2)}$. The optimizing function runs until the resulting value of $\overline{R_0}(\beta)$ does not get closer to the target value.

Table S1.3. Hospitalization parameters

Parameters	Value	Source
γ^H : recovery rate in hospitalized compartment	0.0869565	11.5 day-average from admission to discharge [14]
YHR: symptomatic case hospitalization rate (%)	Overall: [0.04872107, 0.04872107, 3.28757227, 11.33739519, 17.73306336] Low risk: [0.0279, 0.0215, 1.3215, 2.8563, 3.3873] High risk: [0.2791, 0.2146, 13.2154, 28.5634, 33.8733]	Age adjusted from Verity et al. [5]
π : rate of symptomatic individuals go to hospital, age-specific	$\pi = \frac{\gamma^Y \cdot YHR}{\eta+(\gamma^Y-\eta)YHR}$	
η : rate from symptom onset to hospitalized	0.1695	5.9 day average from symptom onset to hospital admission Tindale et al. [15]
μ : rate from hospitalized to death	0.0892857	11.2 day-average from admission to death [14]
HFR: hospitalized fatality ratio, age specific (%)	[4, 12.365, 3.122, 10.745, 23.158]	$HFR = \frac{IFR}{YHR(1-\tau)}$
ν : death rate on hospitalized individuals, age specific	[0.0390, 0.1208, 0.0304, 0.1049, 0.2269]	$\nu = \frac{\gamma^H HFR}{\mu+(\gamma^H-\mu)HFR}$
ICU: proportion hospitalized people in ICU	[0.15, 0.20, 0.15, 0.20, 0.15]	CDC COVID-19 planning scenarios (based on US seasonal flu data)
Vent: proportion of individuals in ICU needing ventilation	[0.35, 0.3, 0.45, 0.5, 0.45]	CDC planning scenarios (based on US seasonal flu data)

d_{ICU} : duration of stay in ICU	8 days	Assumption, computed as average of hospital stay and ventilation durations
d_V : duration of ventilation	5 days	CDC COVID-19 planning scenarios
HCS: healthcare capacity	Hospital bed: 4299 ICU bed: 755 Ventilator: 755	Estimates provided by each of the region's hospital systems and aggregated by regional public health leaders

Table S1.4. Home contact matrix (daily number contacts by age group at home)

	0-4y	**5-17y**	**18-49y**	**50-64y**	**65y+**
0-4y	0.5	0.9	2.0	0.1	0.0
5-17y	0.2	1.7	1.9	0.2	0.0
18-49y	0.2	0.9	1.7	0.2	0.0
50-64y	0.2	0.7	1.2	1.0	0.1
65y+	0.1	0.7	1.0	0.3	0.6

Table S1.5. School contact matrix (daily number contacts by age group at school)

	0-4y	**5-17y**	**18-49y**	**50-64y**	**65y+**
0-4y	1.0	0.5	0.4	0.1	0.0
5-17y	0.2	3.7	0.9	0.1	0.0
18-49y	0.0	0.7	0.8	0.0	0.0
50-64y	0.1	0.8	0.5	0.1	0.0
65y+	0.0	0.0	0.1	0.0	0.0

Table S1.6. Work contact matrix (daily number contacts by age group at work)

	0-4y	5-17y	18-49y	50-64y	65y+
0-4y	0.0	0.0	0.0	0.0	0.0
5-17y	0.0	0.1	0.4	0.0	0.0
18-49y	0.0	0.2	4.5	0.8	0.0
50-64y	0.0	0.1	2.8	0.9	0.0
65y+	0.0	0.0	0.1	0.0	0.0

Table S1.7. Others contact matrix (daily number contacts by age group at other locations)

	0-4y	5-17y	18-49y	50-64y	65y+
0-4y	0.7	0.7	1.8	0.6	0.3
5-17y	0.2	2.6	2.1	0.4	0.2
18-49y	0.1	0.7	3.3	0.6	0.2
50-64y	0.1	0.3	2.2	1.1	0.4
65y+	0.0	0.2	1.3	0.8	0.6

Section S2. Estimation of age-stratified proportion of population at high-risk for COVID-19 complications

We estimate age-specific proportions of the population at high risk of complications from COVID-19 based on data for Austin, TX and Round-Rock, TX from the CDC's 500 cities project (Fig. S2) [16]. We assume that high risk conditions for COVID-19 are the same as those specified for influenza by the CDC [9]. The CDC's 500 cities project provides city-specific estimates of prevalence for several of these conditions among adults.[17] The estimates were obtained from the 2015-2016 Behavioral Risk Factor Surveillance System (BRFSS) data using a small-area estimation methodology called multi-level regression and poststratification [10,11]. It links geocoded health surveys to high spatial resolution population demographic and socioeconomic data [11].

Estimating high-risk proportions for adults. To estimate the proportion of adults at high risk for complications, we use the CDC's 500 cities data, as well as data on the prevalence of HIV/AIDS, obesity and pregnancy among adults (Table S2.1).

The CDC 500 cities dataset includes the prevalence of each condition on its own, rather than the prevalence of multiple conditions (e.g., dyads or triads). Thus, we use separate co-morbidity estimates to determine overlap. Reference about chronic conditions [18] gives US estimates for the proportion of the adult population with 0, 1 or 2+ chronic conditions, per age group. Using this and the 500 cities data we can estimate the proportion of the population p_{HR} in each age group in each city with at least one chronic condition listed in the CDC 500 cities data (Table S2.1) putting them at high-risk for flu complications.

HIV: We use the data from table 20a in CDC HIV surveillance report [19] to estimate the population in each risk group living with HIV in the US (last column, 2015 data). Assuming independence between HIV and other chronic conditions, we increase the proportion of the population at high-risk for influenza to account for individuals with HIV but no other underlying conditions.

Morbid obesity: A BMI over 40kg/m^2 indicates morbid obesity and is considered high risk for influenza. The 500 Cities Project reports the prevalence of obese people in each city with BMI over 30kg/m^2 (not necessarily morbid obesity). We use the data from table 1 in Sturm and Hattori [20] to estimate the proportion of people with BMI>30 that actually have BMI>40 (across the US); we then apply this to the 500 Cities obesity data to estimate the proportion of people who are morbidly obese in each city. Table 1 of Morgan et al. [21] suggests that 51.2% of morbidly obese adults have at least one other high risk chronic condition, and update our high-risk population estimates accordingly to account for overlap.

Pregnancy: We separately estimate the number of pregnant women in each age group and each city, following the methodology in CDC reproductive health report [22]. We assume independence between any of the high-risk factors and pregnancy, and further assume that half the population are women.

Estimating high-risk proportions for children. Since the 500 Cities Project only reports data for adults 18 years and older, we take a different approach to estimating the proportion of children at high risk for severe influenza. The two most prevalent risk factors for children are asthma and obesity; we also account for childhood diabetes, HIV and cancer.

From Miller et al. [23], we obtain national estimates of chronic conditions in children. For asthma, we assume that variation among cities will be similar for children and adults. Thus, we use the relative prevalence of asthma in adults to scale our estimates for children in each city. The prevalence of HIV and cancer in children are taken from CDC HIV surveillance report [19] and cancer research report [24], respectively.

We first estimate the proportion of children having either asthma, diabetes, cancer or HIV (assuming no overlap in these conditions). We estimate city-level morbid obesity in children using the estimated morbid obesity in adults multiplied by a national constant ratio for each age group estimated from Hales et al. [25], this ratio represents the prevalence in morbid obesity in children given the one observed in adults. From Morgan et al. [21], we estimate that 25% of morbidly obese children have another high-risk condition and adjust our final estimates accordingly.

Resulting estimates. We compare our estimates for the Austin-Round Rock Metropolitan Area to published national-level estimates [26] of the proportion of each age group with underlying high risk conditions (Table S2.2). The biggest difference is observed in older adults, with Austin having a lower proportion at risk for complications for COVID-19 than the national average; for 25-39 year-old the high risk proportion is slightly higher than the national average.

Fig S2. Demographic and risk composition of the Austin-Round Rock population

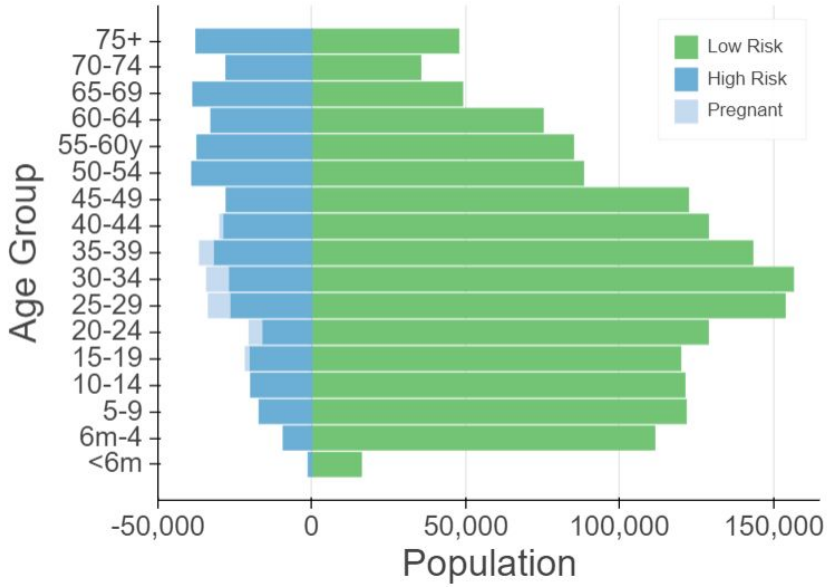

Bars indicate age-specific population sizes, separated by low risk, high risk, and pregnant. High risk is defined as individuals with cancer, chronic kidney disease, COPD, heart disease, stroke, asthma, diabetes, HIV/AIDS, and morbid obesity, as estimated from the CDC 500 Cities Project [16], reported HIV prevalence [19] and reported morbid obesity prevalence [20,21], corrected for multiple conditions. The population of pregnant women is derived using the CDC's method combining fertility, abortion and fetal loss rates [27–29].

Table S2.1. High-risk conditions for influenza and data sources for prevalence estimation

Condition	Data source
Cancer (except skin)	CDC 500 cities [16]
Chronic kidney disease	CDC 500 cities [16]
COPD	CDC 500 cities [16]
Coronary heart disease	CDC 500 cities [16]
Stroke	CDC 500 cities [16]
Asthma	CDC 500 cities [16]

Diabetes	CDC 500 cities [16]
HIV/AIDS	CDC HIV Surveillance report [19]
Obesity	CDC 500 cities complemented with Sturm and Hattori[20] and Morgan et al. [21]
Pregnancy	National Vital Statistics Reports [27] and abortion data [28]

Table S2.2. Comparison between published national estimates and Austin-Round Rock MSA estimates of the percent of the population at high-risk of influenza/COVID-19 complications

Age Group	National estimates[25]	Austin (excluding pregnancy)	Pregnant women (proportion of age group)
0 to 6 months	NA	6.8	-
6 months to 4 years	6.8	7.4	-
5 to 9 years	11.7	11.6	-
10 to 14 years	11.7	13.0	-
15 to 19 years	11.8	13.3	1.7
20 to 24 years	12.4	10.3	5.1
25 to 34 years	15.7	13.5	7.8
35 to 39 years	15.7	17.0	5.1
40 to 44 years	15.7	17.4	1.2
45 to 49 years	15.7	17.7	-
50 to 54 years	30.6	29.6	-
55 to 60 years	30.6	29.5	-
60 to 64 years	30.6	29.3	-
65 to 69 years	47.0	42.2	-
70 to 74 years	47.0	42.2	-
75 years and older	47.0	42.2	-

Section S3. Sensitivity analysis with respect to healthcare durations

With the assumption that the healthcare system is likely to perform less effectively under the highly stressed condition, patient discharge may take longer in the surge setting. As sensitivity analysis, we analyzed longer duration hospital, ICU and ventilator treatment (Table S3.1). The results are summarized in Tables S3.2 and S3.3 and Fig. S3.

Table S3.1. Updated Hospitalization Parameters. All values were modified based on discussions with Austin-Round Rock Medical authorities regarding worst case surge scenarios.

Parameters	Original	Updated for sensitivity analysis	Details
γ^H: recovery rate in hospitalized compartment	0.0869565	0.07142857	14 day average from admission to discharge.
μ: rate from hospitalized to death	0.0892857	0.07142857	14 day average from admission to death
Vent: proportion of individuals in ICU needing ventilation	[0.35, 0.3, 0.45, 0.5, 0.45]	[0.67, 0.67, 0.67, 0.67, 0.67]	
d_{ICU} : duration of stay in ICU	8 days	14 days	
d_V : duration of ventilation	5 days	10 days	

Table S3.2. Longer treatment surge scenario: estimated cumulative COVID-19 cases, healthcare requirements and deaths. The values are medians across 100 stochastic simulations for the Austin-Round Rock MSA from March 1 through August 17, 2020 based on the parameters given in Table S3.1.

Outcomes	No measures	School closure	School closure + 50% social distancing	School closure + 75% social distancing	School closure + 90% social distancing
Hospitalizations	87,851	86,744	62,241	19,376	3,041
ICU	14,713	1,4528	10,451	3,257	512
Ventilators	9,808	9,685	6,967	2,171	342

Table S3.3. Longer treatment surge scenario: estimated peak COVID-19 healthcare demands. The values are medians across 100 stochastic simulations for the Austin-Round Rock MSA from March 1 through August 17, 2020 based on the parameters given in Table S3.1.

Outcomes	No measures	School closure	School closure + 50% social distancing	School closure + 75% social distancing	School closure + 90% social distancing
Hospitalizations	21,152	20,308	14,893	7,238	1,152
ICU	3,556	3,410	2,498	1,217	195
Ventilators	1,693	1,624	1,189	579	93

Fig S3. Longer treatment surge scenario: projected COVID-19 healthcare demand and cumulative deaths in the Austin-Round Rock MSA from March 1 to August 17, 2020

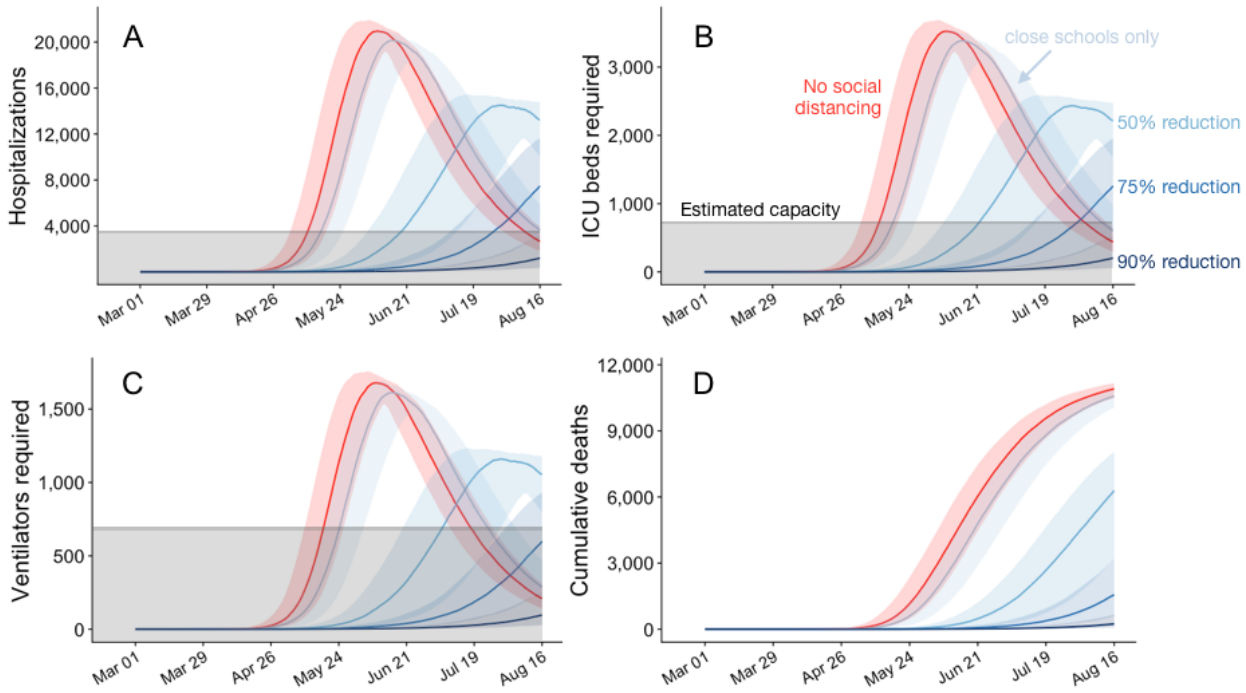

Graphs show simulation results across multiple levels of social distancing, assuming R_0=2.2 with a four-day epidemic doubling time. Extensive social distancing is expected to substantially reduce the burden of COVID-19 (A) hospitalizations, (B) patients requiring ICU care, (C) patients requiring mechanical ventilation and (D) mortality. The red lines project COVID-19 transmission assuming no interventions under the parameters given in Table S1. The blue lines show increasing levels of social distancing interventions, from light to dark: school closures plus social distancing interventions that reduce non-household contacts by either 0%, 50%, 75% or 90%. Lines and shading indicate the median and inner 95% range of values across 100 stochastic simulations. Gray shaded region indicates estimated surge capacity for COVID-19 patients in the Austin-Round Rock MSA as of March 28, 2020, which is calculated based on 80% of the total 4299 hospital beds and 90% of the total 755 ICU beds and 755 mechanical ventilators.

Section S4. Impact of two-week and four-week delays in implementation of social distancing interventions

Our base scenarios assume that social distancing measures are implemented on March 14 or May 14, 2020. We also modeled intermediate delays of two weeks (March 28) and four weeks (April 11). Even two-week delays undermine the efficacy of the interventions with respect to reducing healthcare demand below local capacity (Fig. S4 and Table S4).

Fig S4. Delayed implementation of social distancing measures: projected COVID-19 ICU requirements in the Austin-Round Rock MSA from March 14 to August 17, 2020

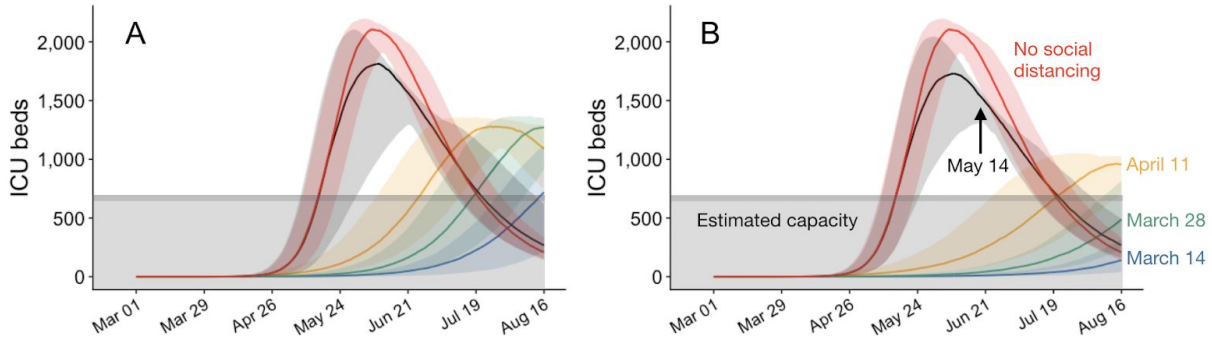

Graphs show simulation results for school closures with (A) 75% reduction in non-household contacts and (B) 90% reduction in non-household contacts, assuming R_0=2.2 with a four-day epidemic doubling time. The red lines project COVID-19 transmission assuming no interventions under the parameters given in Table S1. The other lines colors indicate different delays in the timing of intervention: blue, green, yellow and black correspond to March 14, March 28, April 11, and May 14, 2020, respectively. Lines and shading indicate the median and inner 95% range of values across 100 stochastic simulations. Gray shaded region indicates estimated surge capacity for COVID-19 patients in the Austin-Round Rock MSA as of March 28, 2020, which is calculated based on 90% of the total 755 ICU beds.

Table S4. Date when COVID-19 healthcare requirements exceed capacity based on implementation date for school closures with 75% or 90% social distancing. Each value is a median across 100 stochastic simulations for the Austin-Round Rock MSA prior to August 17, 2020, based on the parameters given in Table S1.

Outcomes	School closure + 75% social distancing			School closure + 90% social distancing		
	March 14 start	March 28 start	April 11 start	March 14 start	March 28 start	April 11 start
Hospitalizations	August 1	July 7	June 15	Not exceed	August 12	July 4
ICU	Aug 15	July 18	June 26	Not exceed	Not exceed	July 21

References

1. Keeling MJ, Rohani P. Modeling Infectious Diseases in Humans and Animals. Princeton University Press; 2011.

2. Gillespie DT. Approximate accelerated stochastic simulation of chemically reacting systems. J Chem Phys. 2001;115: 1716–1733.

3. Li Q, Guan X, Wu P, Wang X, Zhou L, Tong Y, et al. Early Transmission Dynamics in Wuhan, China, of Novel Coronavirus-Infected Pneumonia. N Engl J Med. 2020. doi:10.1056/NEJMoa2001316

4. Kraemer MUG, Yang C-H, Gutierrez B, Wu C-H, Klein B, Pigott DM, et al. The effect of human mobility and control measures on the COVID-19 epidemic in China. medRxiv. 2020. Available: https://www.medrxiv.org/content/10.1101/2020.03.02.20026708v1

5. Verity R, Okell LC, Dorigatti I, Winskill P, Whittaker C, Imai N, et al. Estimates of the severity of COVID-19 disease. Epidemiology. medRxiv; 2020. doi:10.1101/2020.03.09.20033357

6. Mizumoto K, Kagaya K, Zarebski A, Chowell G. Estimating the Asymptomatic Proportion of 2019 Novel Coronavirus onboard the Princess Cruises Ship, 2020. Infectious Diseases (except HIV/AIDS). medRxiv; 2020. doi:10.1101/2020.02.20.20025866

7. Lauer SA, Grantz KH, Bi Q, Jones FK, Zheng Q, Meredith HR, et al. The Incubation Period of Coronavirus Disease 2019 (COVID-19) From Publicly Reported Confirmed Cases: Estimation and Application. Ann Intern Med. 2020. doi:10.7326/M20-0504

8. Du Z, Xu X, Wu Y, Wang L, Cowling BJ, Meyers LA. The serial interval of COVID-19 from publicly reported confirmed cases. Epidemiology. medRxiv; 2020. doi:10.1101/2020.02.19.20025452

9. CDC. People at High Risk of Flu. In: Centers for Disease Control and Prevention [Internet]. 1 Nov 2019 [cited 26 Mar 2020]. Available: https://www.cdc.gov/flu/highrisk/index.htm

10. CDC - BRFSS. 5 Nov 2019 [cited 26 Mar 2020]. Available: https://www.cdc.gov/brfss/index.html

11. Zhang X, Holt JB, Lu H, Wheaton AG, Ford ES, Greenlund KJ, et al. Multilevel regression and poststratification for small-area estimation of population health outcomes: a case study of chronic obstructive pulmonary disease prevalence using the behavioral risk factor surveillance system. Am J Epidemiol. 2014;179: 1025–1033.

12. Calendar of Events. In: Austin ISD [Internet]. [cited 26 Mar 2020]. Available: https://www.austinisd.org/calendar

13. minimize(method='trust-constr') — SciPy v1.4.1 Reference Guide. [cited 28 Mar 2020]. Available: https://docs.scipy.org/doc/scipy/reference/optimize.minimize-trustconstr.html

14. Sanche S, Lin YT, Xu C, Romero-Severson E, Hengartner N, Ke R. The Novel Coronavirus, 2019-nCoV, is Highly Contagious and More Infectious Than Initially Estimated. Epidemiology. medRxiv; 2020. doi:10.1101/2020.02.07.20021154

15. Tindale L, Coombe M, Stockdale JE, Garlock E, Lau WYV, Saraswat M, et al. Transmission interval estimates suggest pre-symptomatic spread of COVID-19. Epidemiology. medRxiv; 2020. doi:10.1101/2020.03.03.20029983

16. 500 Cities Project: Local data for better health | Home page | CDC. 5 Dec 2019 [cited 19 Mar 2020]. Available: https://www.cdc.gov/500cities/index.htm

17. Health Outcomes | 500 Cities. 25 Apr 2019 [cited 28 Mar 2020]. Available: https://www.cdc.gov/500cities/definitions/health-outcomes.htm

18. Part One: Who Lives with Chronic Conditions. In: Pew Research Center: Internet, Science & Tech [Internet]. 26 Nov 2013 [cited 23 Nov 2019]. Available: https://www.pewresearch.org/internet/2013/11/26/part-one-who-lives-with-chronic-conditions/

19. for Disease Control C, Prevention, Others. HIV surveillance report. 2016; 28. URL: http://www cdc gov/hiv/library/reports/hiv-surveil-lance html Published November. 2017.

20. Sturm R, Hattori A. Morbid obesity rates continue to rise rapidly in the United States. Int J Obes . 2013;37: 889–891.

21. Morgan OW, Bramley A, Fowlkes A, Freedman DS, Taylor TH, Gargiullo P, et al. Morbid obesity as a risk factor for hospitalization and death due to 2009 pandemic influenza A(H1N1) disease. PLoS One. 2010;5: e9694.

22. Estimating the Number of Pregnant Women in a Geographic Area from CDC Division of Reproductive Health. Available: https://www.cdc.gov/reproductivehealth/emergency/pdfs/PregnacyEstimatoBrochure508.pdf

23. Miller GF, Coffield E, Leroy Z, Wallin R. Prevalence and Costs of Five Chronic Conditions in

Children. J Sch Nurs. 2016;32: 357–364.

24. Cancer Facts & Figures 2014. [cited 30 Mar 2020]. Available: https://www.cancer.org/research/cancer-facts-statistics/all-cancer-facts-figures/cancer-facts-figures-2014.html

25. Hales CM, Fryar CD, Carroll MD, Freedman DS, Ogden CL. Trends in Obesity and Severe Obesity Prevalence in US Youth and Adults by Sex and Age, 2007-2008 to 2015-2016. JAMA. 2018;319: 1723–1725.

26. Zimmerman RK, Lauderdale DS, Tan SM, Wagener DK. Prevalence of high-risk indications for influenza vaccine varies by age, race, and income. Vaccine. 2010;28: 6470–6477.

27. Martin JA, Hamilton BE, Osterman MJK, Driscoll AK, Drake P. Births: Final Data for 2017. Natl Vital Stat Rep. 2018;67: 1–50.

28. Jatlaoui TC, Boutot ME, Mandel MG, Whiteman MK, Ti A, Petersen E, et al. Abortion Surveillance - United States, 2015. MMWR Surveill Summ. 2018;67: 1–45.

29. Ventura SJ, Curtin SC, Abma JC, Henshaw SK. Estimated pregnancy rates and rates of pregnancy outcomes for the United States, 1990-2008. Natl Vital Stat Rep. 2012;60: 1–21.